

1 **Phytoremediation of highly contaminated mining soils by *Jatropha***
2 ***curcas* L and production of catalytic carbons from the generated**
3 **biomass**

4
5 Paloma Álvarez-Mateos, Francisco-Javier Alés-Álvarez, Juan Francisco García-Martín *

6 Department of Chemical Engineering, Faculty of Chemistry, University of Seville, C/

7 Profesor García González, 1, 41012 Seville, Spain

8 *Corresponding author. *E-mail address*: jfgarmar@us.es

9

10

11 **Abstract**

12 This paper deals with the removal of heavy metals from marginal soil mixtures from the
13 Cobre Las Cruces and Aznalcóllar mining areas containing high concentrations of metals
14 (Cr, Fe, Ni, Cu, Zn, Cd, Hg, Pb and As) by means of phytoremediation using *Jatropha*
15 *curcas* L., and the subsequent production of biocatalysts from the plant biomass. First, *J.*
16 *curcas* L. was sowed in eight mixtures of these mining soils to study its adaption to these
17 high-contaminated soils and its growth during 60 days in a greenhouse under conditions
18 simulating the South of Spain's spring climate. Later, the most suitable soil mixtures for
19 plant growth were used for 120-day phytoremediation under the same conditions. Heavy
20 metal concentration in soils, roots, stems and leaves were measured by ICP-OES at the
21 beginning, at the middle and at the end of the phytoremediation period, thus calculating
22 the translocation and bioaccumulation factors. *J. curcas* L. was found to absorb great
23 amounts of Fe (> 3000 mg kg⁻¹ plant) as well as notable amounts of Pb, Zn, Cu, Cr and
24 Ni, and traces of As. Other metals with lower initial concentrations such as Cd, Hg and
25 Sn were completely removed from soils. Finally, the plant biomass was subjected to

26 pyrolysis to obtain catalytic biocarbons, assessing the optimal temperature for the
27 pyrolytic process by means of thermogravimetric analysis and Raman spectroscopy.

28

29 *Keywords:* bioaccumulation; *Jatropha curcas*; mining soils; phytoremediation;
30 translocation factor.

31

32 **Introduction**

33 Soil contamination by heavy metals (As, Cd, Cr, Cu, Pb and Zn) is one of the major
34 environmental problems raising critical concerns for both human health and ecosystems
35 (Singh et al., 2011) due to their carcinogenic and mutagenic effects on animals and
36 humans (Sánchez-Chardi et al., 2009). Small quantities of these metals are required for
37 human health, however in higher concentrations they become toxic or dangerous,
38 affecting brain, kidney, lungs, liver and other important organs. Moreover, long-term
39 exposure to them can cause physical, muscular and neurological degenerative processes,
40 and even cancer (Järup, 2003). The clean-up of most of these soils is mandatory for the
41 area to be reclaimed and to minimize the entry of potentially toxic elements into the food
42 chain.

43 The main anthropogenic sources of heavy metals in soils are related to the mining
44 industry. The mining sector produces a whole range of gaseous pollutants both solid and
45 liquid. This can occur in different ways: by deposition from the atmosphere as sediment
46 particles or brought by rainwater; by direct discharge of the liquid products of mining and
47 metallurgical activity; or by infiltration of leachate from the mining environment.
48 Specifically, mining and mineral processing of sulphide ore deposits produce large
49 quantities of wastes, most of which are regarded as toxic or hazardous, due to the

50 formation of acid drainage, and to their heavy metal content (Jiménez-Moraza et al.,
51 2006).

52 Phytoremediation basically refers to the use of plants and associated soil microbes to
53 reduce the concentrations or toxic effects of contaminants in the environment (Singh et
54 al., 2003; Suresh and Ravishankar, 2004). It can be used for the removal of not only heavy
55 metals but also organic pollutants such as polynuclear aromatic hydrocarbons,
56 polychlorinated biphenyls and pesticides.

57 Phytoremediation employs on-site plants to absorb heavy metals and to prevent their
58 further transport. Plants generally handle the contaminants without affecting topsoil, thus
59 conserving its utility and fertility. They may improve soil fertility and increase organic
60 matter content (Abhilash et al., 2012; Cobbett, 2003). Therefore, phytoremediation is an
61 environmental ecotechnology that can be applied to remediate contaminated soils. It is a
62 novel, cost-effective, efficient, environmental and eco-friendly remediation strategy that
63 can be applied *in situ* and is solar-driven (LeDuc and Terry, 2005; Mukhopadhyay and
64 Maiti, 2010). What is more, it has already been demonstrated that phytoremediation is a
65 more ecological and economic technique than the conventional physical-chemical
66 alternatives (González-Chávez and Carrillo-González, 2013).

67 Recently, it has been reported that *Jatropha curcas* L. has a high capacity for
68 bioaccumulation, phytotranslocation and phytoremediation of heavy metals (Chang et al.,
69 2014; González-Chávez et al., 2017; Marrugo-Negrete et al., 2015). *J. curcas* L. is a plant
70 belonging to the Euphorbiaceae family. It is cultivated in tropical and subtropical regions
71 around the world, becoming naturalized in some areas (Jamil et al., 2009; Pandey et al.,
72 2012). This plant survives and grows on marginal, eroded and depleted lands. It requires
73 little water to grow, although it does not tolerate heavy rains. The implementation of these
74 fast growing plants in degraded or contaminated areas is important for improving soil

75 quality and preventing erosion. It also leads to organic matter enrichment and to greater
76 diversity of microorganisms in the soil (Abhilash et al., 2013). This plant can also
77 accumulate most metallic elements in quantities of up to 0.01% of its dry weight (1000
78 mg kg⁻¹) (Ahmadpour et al., 2014; Ghavri and Singh, 2010). Other studies have shown
79 that Cr, Hg and Pb are not easily transferred to aerial plant biomass as they are mainly
80 stored in root cells (Bernabé-Antonio et al., 2015; Marrugo-Negrete et al., 2015), while
81 Zn is easily accumulated in green tissues (Yadav et al., 2009).

82 Although phytoremediation is a promising approach for the recovery of soils
83 contaminated with heavy metals, its main drawback is the later use of the contaminated
84 biomass generated over phytoremediation. As soon as the plants have absorbed the
85 pollutants from the soil, it is necessary to withdraw them from the contaminated zone.
86 The contaminated plants are regarded as residues and are kept in vegetable containers so
87 the problem is not solved.

88 The implementation of these fast growing plants in degraded or contaminated areas is
89 important for the soil quality, erosion prevention as well as organic matter enrichment
90 and diversity of microorganisms in soil. In addition to the beneficial effects on the soil,
91 the biomass obtained from *J. curcas* L. (stems, leaves and roots) could be used as a
92 potential source of energy and other resources (Chavan et al., 2015; Teo et al., 2015,
93 2014). A potential alternative is to perform thermochemical processes such as pyrolysis
94 to transform this biomass into high added-value products. Pyrolysis is a process for which
95 a material is thermally decomposed in the absence of oxygen or any other oxidizing agent.
96 The principal product obtained in the pyrolysis is pyrolytic carbon, which has numerous
97 potential applications, such as its use as acid heterogeneous catalysts (Yee et al., 2011).
98 Its properties depend mainly on the biomass composition, reactor type and the
99 experimental conditions in which pyrolysis is performed.

100 In the present work, we have studied the growth and adaptation of *J. curcas* L. to highly
101 contaminated soils by heavy metals under the climatic conditions of the South of Spain
102 as well as the phytoremediation capacity (extraction of heavy metals from soil) of *J.*
103 *curcas* L. The distribution of extracted heavy metals in roots, stems and leaves was
104 analysed and quantified by ICP-OES. Bioaccumulation or bioconcentration factors (BAF)
105 and translocation factors (TF) of heavy metals were also compared. Finally, we have
106 assayed the formation of biocarbons, with catalytic properties, from *J. curcas* L. roots,
107 determining the structure of the biocarbons by Raman spectroscopy.

108

109 **2. Materials and methods**

110 **2.1. Soil samples from the mining land**

111 Soil samples were collected in Cobre Las Cruces and Aznalcóllar mining areas in
112 Andalusia, in the South of Spain.

113 In Cobre Las Cruces mine, 300 kg were taken from the storage zone for the original
114 topsoil in the mining region (Fig. S1.A). This soil (NCS) is currently used for the
115 subsequent restoration of the landscape and to minimize the visual impact of the mine.

116 In Aznalcóllar mine, samples were taken from the heap area with the highest
117 concentration of leachate metals. Two zones of well-differentiated soils were found in
118 this mine (Fig. S1.B and S1.C). One with yellow soil (YCS) and another one with grey
119 soil (GCS), so both samples were taken. A surface area of 50 m² was selected placing an
120 imaginary mesh with 5 m sides (i.e. two adjacent 25-m² grids for each soil). 5-kg samples
121 were taken at the centre of each grid at three different depths (0 – 30 cm, 30 – 60 cm and
122 60 – 90 cm, respectively, from the surface), which were subsequently mixed and
123 homogenized in a mixer for one hour.

124 Finally, the three soils were transported to a greenhouse. After their analysis, they were
125 used as substrate for the trials.

126 **2.2. Germination of *Jatropha curcas* L. seeds**

127 Seventy *J. curcas* L. seeds from Argentina were sown in vermiculite in 8-cm diameter
128 pots. They were germinated in a Fitoclima 18000EH climate chamber (Aralab, Portugal)
129 under the following conditions: 25 °C, 80% humidity and continuous lighting (Fig. S1.D).

130 The plants were watered with Hoagland solution containing (in mmol L⁻¹) 6.0 KNO₃, 4.0
131 Ca(NO₃)₂·4H₂O, 2.0 NH₄H₂PO₄, 1.0 MgSO₄·7H₂O, 50.0 KCl, 25.0 H₃BO₃, 2.0
132 MnSO₄·H₂O, 2.0 ZnSO₄·7H₂O, 0.5 CuSO₄·5H₂O, 0.5 H₂MoO₄, and 20.0 Fe-EDTA,
133 providing K, Ca, N and P, Mg, Cl, B, Mn, Cl, B, Mn, Zn, Cu, Mo, and Fe, respectively.

134 Sixty seeds germinated, 85% of all those planted. The seedlings were kept in this climate
135 chamber for about 6 weeks until they were 25 cm tall (Fig. S1.E). Immediately afterwards
136 they were planted into 20-cm diameter plant pots containing peat moss (Universal Compo
137 Sana Substrate, Germany) and placed in a greenhouse. The climate in the greenhouse
138 simulated that of spring in the South of Spain; that is, a daytime temperature of 25 ± 3 °C
139 and 18 ± 3 °C at night, 60% humidity and between 8 and 14 h of light. The plants were
140 kept under these conditions for about six weeks to acclimate before the beginning of both
141 adaptation and absorption trials in mine soils, the resulting plant tall being 70 – 90 cm
142 (Fig. S1.F).

143 **2.3. Preliminary assessment of *Jatropha curcas* L. adaptation to contaminated soils**

144 First, the study of the adaptation of *J. curcas* L. to the three soils was made. Eight mixtures
145 of soils were assayed (Table 1), 5 replicas of each trial being performed. Plants were let
146 to grow in these soils for 60 days, being watered with tap water once a week. For further
147 comparison, 5 plants were sown in vermiculite (V100) and watered with Houlang
148 solution. Another 5 plants were analysed at day 0 as reference. Visual observations and

149 pH measures were carried out at days 0, 7, 14 and 60. Chemical analysis of the soil
150 mixtures as well as of the plant biomass (roots, stems and leaves) were performed at the
151 beginning and at the end of this adaptation period.

152 **2.4. Heavy metal absorption trials**

153 Three of the soil mixtures assayed in the adaptation trials, namely NCS100, YCS20 and
154 YCS50, were selected to assess the heavy metal absorption by *J. curcas* L. Plants were
155 sowed in 50-cm diameter pots and were let to grow for 120 days, being watered with tap
156 water once a week. Ten replicas of each trial were performed. Five replicas of soils and
157 plants were analysed after 60 days (first cut-off) and another 5 replicas after 120 days
158 (second cut-off).

159 **2.5. Catalytic carbons production**

160 The dried and sieved roots of the plants were subjected to pyrolysis in an inert nitrogen
161 atmosphere at 300, 350, 400, 450, 500, 550, 600, 650 and 700 °C, respectively. To do
162 this, 0.5 g sample were placed in a 25 x 300 quartz tube and introduced in a Carbolite
163 Tube Furnace MTF 12/38/250 equipped with a Eurotherm 2416CG temperature
164 controller. The outlet of the quartz tube was connected to two bubblers submerged in ice
165 to condense the flue gases (bio-oils), an extractor hood eliminating the uncondensed
166 gases. The flow of inert N₂ gas was set to 6 L h⁻¹, and the heating rate was set to 30 °C
167 min⁻¹. The working temperature was maintained for 2 h. The resulting catalytic carbons
168 were let to cool to room temperature.

169 **2.6. Soil and plant analysis**

170 Before being analysed, soils were weighted and dried in a stove at 60 °C for 72 h. Once
171 dried, the samples were sieved using a 2 mm mesh, removing pebbles but not the clots of
172 soil. A mortar was used to reduce the size of the soil particles and to press them through
173 the sieve. After being sieved, samples were carefully homogenized.

174 As for plant analysis, they were first cut-up, separating roots, stems and leaves. Next, all
175 the parts of the plants were dried in a stove at 60 °C to constant weight. Finally, they were
176 ground using a Culatti DFH48 mill with a 2 mm sieve.

177 **2.6.1. pH**

178 To measure the pH of the soils, 10 g soil were weighed in a beaker and distilled water
179 was added until a thick, homogeneous paste was obtained with no excess water. This was
180 let to stand for 30 min before introducing the pH meter electrode to measure the pH (Ali
181 et al., 2011).

182 **2.6.2. Phosphates**

183 The Olsen method was used to determine the amount of phosphates (PO_4^{3-} or HPO_4^{2-}) in
184 the soil samples. Using this method, it is possible to determine the phosphates that a plant
185 can assimilate. It is based on a colorimetric assay which measures the optical density of
186 the blue solution produced when reducing the phosphomolybdic complex
187 $((\text{NH}_4)\text{PO}_4(\text{MoO}_3)_{12})$ formed by orthophosphoric acid (H_3PO_4) and ammonium
188 molybdate $(\text{NH}_4)\text{MoO}_4$ (Jackson, 1958). Firstly, seven standard solutions from 0.2 to 1
189 mg kg^{-1} KH_2PO_4 were prepared, to which 8 mL 0.03M $(\text{NH}_4)\text{MoO}_4$ solution were added.
190 The absorbance at 880 nm of the resulting solutions was measured in a Varian Cary 100
191 UV-visible spectrophotometer, and a calibration curve was obtained. To analyse
192 phosphates in soil samples, 2.5 g soil were weighed in a beaker, then 50 ml 0.5 N
193 NaHCO_3 were added and the mixture was stirred for 30 min before filtering. Finally, 8
194 mL 0.03M $(\text{NH}_4)\text{MoO}_4$ solution were added to the filtered solution and the absorbance
195 at 880 nm was measured. Results were expressed as mg available phosphorus kg^{-1} soil.

196 **2.6.3. Organic matter**

197 The organic matter in soil samples was determined by oxidising it with potassium
198 dichromate ($\text{K}_2\text{Cr}_2\text{O}_7$) and sulphuric acid (H_2SO_4), measuring the reduced chromium

199 (Cr³⁺) by UV-Vis absorption spectroscopy (Jackson, 1958). Before analysing the
200 samples, a calibration curve was made. Six standard solutions of glucose were prepared
201 from 5 to 50 mg mL⁻¹, reacting 2 mL of each with 10 mL 0.17 M K₂Cr₂O₇ and 10 mL
202 H₂SO₄. As the rate and intensity of oxidation depend on the amount and kind of organic
203 matter in the samples and the reaction temperature, all the reactions took place in a 100
204 °C water bath for 30 min. The same procedure was followed for the reaction of 0.3 g of
205 each of the soil samples. After preparing the standard reactions and the samples, the
206 absorption spectra were recorded between 400 and 800 nm. Results were expressed in g
207 organic matter kg⁻¹ soil.

208 **2.6.4. Carbonates**

209 The percentage of total carbonates (CaCO₃) in soil samples was determined using a
210 gasometric method known as Bernard's calcimetry. This method involves the indirect
211 measurement of the carbonates in the soil by the gasometric determination of the CO₂
212 released when the carbonates in soil samples react with HCl. To calibrate Bernard's
213 calcimetry, 0.25 g pure CaCO₃ were weighed and were let to react with 5 ml 1:1 HCl
214 solution. The same procedure was followed to determine the carbonates in soil samples.

215 **2.6.5. Nitrates**

216 UV-visible absorption spectrophotometry was used to determine the content in nitrates
217 (NO³⁻) in soil samples, recording the absorption spectra of the samples at 220 nm in a
218 Varian Cary 100 UV-visible spectrophotometer (APHA et al., 2005). The calibration
219 curve was obtained from 10 standard solutions from 0.2 to 5.0 mg kg⁻¹ KNO₃ to which 1
220 mL 1 M HCl was added. To determine the content in nitrates in soil samples, 10 g soil
221 were weighed in a beaker and then 50 mL distilled water were added, the mixture being
222 stirred for 1 h before filtering. Finally, 1 mL 1 M HCl was added to the filtered solution.
223 Results were expressed as mg nitrates kg⁻¹ soil.

224 **2.6.6. Trace elements**

225 For the analysis of the trace elements, both soil and plant samples were digested with
226 concentrated HNO₃ and H₂O₂ in a microwave digester (Milestone Ethos One). After
227 digestion, the amount of trace elements in samples was determined using a Horiba Jobin
228 Yvon ICP-OES with automatic Horiba Jobin Yvon AS 500 sampler, a hydride generator
229 and a CETAC AT+ ultrasonic nebulizer.

230 **2.6.7. Elemental analysis**

231 A LECO CHNS 932 elemental analyser, with a Sartorius M2P microbalance, was used to
232 determine the C, N and H percentages in plant samples. This method is based on the
233 complete and instant oxidation of the sample by means of combustion with pure oxygen
234 at temperature varying between 100 and 1000 °C.

235 **2.6.8. Translocation factor (TF) and bioaccumulation factor (BAF)**

236 Heavy metals translocation in plants was calculated using the translocation factor (TF)
237 defined as follows:

238
$$TF = C_{\text{aerial}}/C_{\text{root}} \quad (1)$$

239 where C_{aerial} and C_{root} are metal concentrations (mg kg⁻¹) in the aerial part of the plant
240 (stem and leaves) and root, respectively. Wherein, TF higher than 1 indicates that the
241 plant translocates metals effectively from root to the aerial parts.

242 Furthermore, the bioaccumulation factor (BAF) was also determined by calculating the
243 ratio of metal concentration in the aerial parts to that in the soil:

244
$$BAF = C_{\text{plant_tissue}}/C_{\text{soil}} \quad (2)$$

245 where C_{plant_tissue} is the average metal concentration in the whole plant tissue (mg kg⁻¹)
246 and C_{soil} is metal concentrations in soil (mg kg⁻¹). BAF is used to categorize plants as

247 hyperaccumulators, accumulator and excluder based on the concentration of accumulated
248 metals ($>5 \text{ mg kg}^{-1}$, $>1 \text{ mg kg}^{-1}$ and $<1 \text{ mg kg}^{-1}$, respectively).

249 **2.7. Biocarbons characterization**

250 Raman spectroscopy was used for the structural characterization of the biocarbons. The
251 Raman spectra were recorded using an i-Raman Plus (Microbeam, Spain), equipped with
252 a diode laser emitting at 785 nm as illumination source. The spectrum of a commercial
253 graphite sample (99% carbon), supplied by Schunk Iberica, was also acquired for
254 comparison purpose.

255 **2.8. Statistical analysis**

256 Statistical analysis was carried out with SPSS Statistics 24 (United States) software.
257 Tukey's HSD (honestly significant difference) test in conjunction with an ANOVA (post-
258 hoc analysis) was used to find averages of pH values and contents in heavy metals,
259 carbonates, phosphates, nitrates and organic matter of different contaminated soils, and
260 of heavy metal concentrations of plants sowed in different soils during phytoremediation,
261 that are significantly different from each other ($p \leq 0.05$).

262

263 **3. Results and discussion**

264 **3.1. Analysis of soil samples from Aznalcóllar and Cobre las Cruces mines**

265 The contents of trace elements, carbonates, phosphates, organic matter and nitrates as
266 well as pH were determined in triplicate for GCS, YCS and NCS samples. Table 2 shows
267 the concentration of trace elements in soils from the Cobre las Cruces and Aznalcóllar
268 mines and the maximum values proposed by the Andalusia regional government for a soil
269 to be regarded as contaminated (Simón et al., 1999). The content of Cd, Cu, Zn, Pb, As
270 and Hg in soils from Aznalcóllar mine significantly exceeded the maximum values
271 established for these metals in Andalusia, while Cobre las Cruces mine soil did not. For

272 this reason, the topsoil from Cobre las Cruces mine was labelled as NCS (non-
273 contaminated soil) while soils from the area of exploitation of Aznalcóllar mine were
274 labelled as GCS and YCS (grey and yellow contaminated soil from Aznalcóllar mine,
275 respectively). As for pH, very acidic values were found in the contaminated soils (YCS:
276 1.58 ± 0.08 ; GCS: 0.74 ± 0.02) while the pH of the NCS was close to neutral ($7.47 \pm$
277 0.03), which accounts for the degree of contamination of the Aznalcóllar soils.

278 Taking into account the important role of the presence of iron oxides and hydroxides in
279 the retention of heavy metals and their immobilization, the concentration of this element
280 was calculated in the three types of soils, obtaining 32213, 265357 and 104967 mg kg⁻¹ for
281 NCS, GCS and YCS, respectively. The fact that the concentration of Fe in GCS was two
282 and a half times higher than that in YCS and eight times greater than in NCS is coherent
283 with the high concentrations of trace elements found in both soils from Aznalcóllar mine.
284 The pH of the soil has also influence on the amount of carbonates (CO₃²⁻), phosphates
285 (PO₄³⁻ or HPO₄²⁻), nitrates (NO₃⁻) and organic matter that it contains (Table 3). At low
286 pH, CO₃²⁻ decomposes into CO₂, which accounts for the nil content in GCS and YCS.
287 Besides, soil's microbiological activity is inhibited (Delwiche and Bryan, 1976; Einsle
288 and Kroneck, 2004); this refers to the degradation of the soil's organic matter to obtain
289 energy in the form of mineral nutrients, so the highest organic matter content was found
290 in the soil with the lowest pH (GCS). Bacterial denitrification is also inhibited when pH
291 is below 7, so that nitrates remained in contaminated soils. The optimum pH range for
292 phosphorus absorption by plants is 6.0-7.0. In acidic soils, P tends to react with Fe and
293 Mn, decreasing its availability. This can explain that GCS, the soil with the lowest pH
294 and the highest Fe concentration, had the lowest phosphate content.

295

296 **3.2. Preliminary trials**

297 **3.2.1. *Jatropha curcas* L. adaptation to highly contaminated soils**

298 Once Cobre Las Cruces and Aznalcóllar mines soils were characterised, the first set of
299 trials was carried out to assess whether *J. curcas* L. can adapt and grow in these soils. To
300 do this, the plants that had been germinated in vermiculite were transplanted to 30-cm
301 diameter pots in the soil mixtures defined in Table 1. Visual observations made during 60
302 days indicated that *J. curcas* L. tolerates up to 50% of YCS in the soil mixture. Plants
303 sowed in GCS20 showed wilting of leaves at day 15, and most their leaves had fallen at
304 day 60 (Fig. S2.A). Plants sowed in GCS50, GCS80, YCS80 and GYCS25 presented
305 necrotic leaves at day 15, most of leaves fallen at day 60 (Fig. S2.B). Furthermore, severe
306 necrotic streaks on the stem were observed in plants sowed in GSC80 and YCS80 (Fig.
307 S2.C and S2.D). It is worth noting that *J. curcas* has been demonstrated to grow in mine
308 residue soils with an markedly lower contamination (12 mg Cu kg⁻¹, 184 mg Zn kg⁻¹, 13
309 mg Pb kg⁻¹) with no phytotoxic symptoms (González-Chávez et al., 2017), but this plant
310 has never been tested under the extreme conditions assayed in this work (Table 2). *J.*
311 *curcas* has been found to survive on arsenic, chromium and zinc artificially contaminated
312 soils up to 250, 100 and 3000 mg kg⁻¹, respectively (Yadav et al., 2009), the growth of
313 the plant being inhibited at soil concentrations of 250 mg kg⁻¹ As, 100 mg kg⁻¹ Cr and
314 1000 mg kg⁻¹ Zn. These limits in As and Zn concentrations can be in agreement with our
315 results, based on the plant survival on different soil mixtures and the composition of the
316 original contaminated soils (Table 2). After 60 days, the plants were removed from the
317 pots in order to carry out a complete chemical analysis.

318 **3.2.2. Soil analysis**

319 The pH of the soils was measured over time (Fig. 1). It was observed that the pH of the
320 soils decreased between day 7 and day 15. This could indicate that *J. curcas* L. needs a

321 longer adaptation period to acclimate to the new substrates. From day 15 to the end of the
322 trials the pH raised in the whole soils, but for NCS100. This pH increase was uneven,
323 YCS20 being the soil reaching the maximum pH value (6.5) and with the highest slope.
324 GCS20 and YCS20 were the solely contaminated soils that reached pH higher than 5 and
325 6, respectively, while the final pH values of GCS50, YCS50 and GYCS25 were between
326 3 and 4. On the contrary, the pH values of GCS80 and YCS80 were less than 2. These
327 results are consistent with the anomalies observed in the evolution of the plants (Fig. S2)
328 and it can be concluded that *J. curcas* L. cannot adapt to soils with percentages of
329 contaminated soil of Aznalcóllar mine (either GCS or YCS) greater than 50%.

330 **3.2.3. Analysis of *Jatropha curcas* L. biomass at the end of the adaptation period**

331 The percentages of root, stem and leaf growth, with respect to reference plants analysed
332 at day 0, for each soil after the 60-day adaptation period are illustrated in Fig. 2. The
333 highest growth was found in stems, followed by roots and, finally, leaves. Obviously, the
334 maximum biomass growth was attained in plants sowed in vermiculite and watered with
335 Houlang solution (V100). As can be observed, the increase of GCS in soils resulted in
336 a decrease in stem growth while the increase of YCS in soils led to the opposite effect
337 (Fig. 2). High percentages of GCS or YCS in soils were detrimental to leaves growth.
338 When comparing the growth of plants in soils containing GCS and YSC with that of plants
339 sowed in non-contaminated soil (NSC100), it could be concluded that the presence of
340 metals in contaminated soils is not only non detrimental to plant growth, but also biomass
341 production is favoured to some extent, mainly in mixture soils containing YCS.

342

343 **3.3. Absorption of heavy metals by *Jatropha curcas* L. in contaminated soils**

344 As mentioned earlier, soils containing GCS or percentages of YCS higher than 50% led

345 to serious adaptation problems, resulting in partial or total necrosis of *J. curcas* L., thereby
346 solely NCS100, YCS20 and YCS50 mixture soils were used in heavy metal absorption
347 trials.

348

349 **3.3.1. Analysis of NCS100, YCS20 and YCS50 soils after 60 and 120 days**

350 The analyses carried out at days 0, 60 and 120 showed a pH increase in contaminated
351 soils (YCS20 and YCS50) until reaching equilibrium (Fig. 3), which accounts for the
352 good adaptation of *J. curcas* L. species to these contaminated soils.

353 Regarding macronutrients, the initial soil carbonate content drastically decreased over
354 time (Fig. 4.A), because carbonates neutralize the acid excess caused by the presence of
355 metals, leading to liberation of CO₂ and the increase in the pH (Fig. 3). The concentration
356 of nitrates increased during phytoremediation in the three soils (Fig. 4.B). It could be due
357 to the production of nitrates by nitrification bacteria and the potential inhibition of
358 denitrification bacteria at pH lower than 7. Meanwhile, significant differences were not
359 found for the amounts of phosphates and organic matter in the non-contaminated soil
360 (Fig. 4.C and 4.D). By contrast, the concentration of phosphates increased at day 60 to
361 subsequently decrease at day 120 in YCS20 and YCS50 soils (Fig. 4.C), the phosphates
362 concentration at the end of the phytoremediation period being higher than the initial one.
363 Furthermore, the organic matter content decreased in these contaminated soils (Fig. 4.D)
364 due to low bacteria activity.

365 Table 4 illustrates the percentage of reduction of heavy metals in each soil at the end of
366 the 120-day phytoremediation. Metals such as Cd, Hg and Sn decreased by 100% as a
367 consequence of their low initial concentrations (<10 mg kg⁻¹), while concentrations of
368 metals with initial concentrations between 10 and 1000 mg kg⁻¹ decreased by 30 – 70%,
369 with the exception of As, which agrees with previous results (Tripathi et al., 2007; Yadav

370 et al., 2009). The concentration of Fe decreased by only 15-39% due to its high initial
371 concentration ($> 30000 \text{ mg kg}^{-1}$).

372 **3.3.2. Analysis of the plants sowed in NCS100, YCS20 and YCS50 soils**

373 While differences were hardly observed after 60 days, Fig. 5 clearly shows that the
374 biomass production after 120 days drastically decreased when increasing the percentage
375 of YCS in the soil. Thus, *J. curcas* L. barely grew in YCS50 from day 60 to day 120. The
376 elemental analysis of roots, stems and leaves after 120 days (Fig. 6) showed that the
377 absorption of these metals by the plants affects, above all, the content of N, which
378 increased its percentage in leaves and decreased in roots and stems when increasing the
379 percentage of YCS in the soil where the plant was sowed (Fig. 6.C). The higher
380 percentage of N in YCS20 and YCS50 leaves can be related to the chelating power of
381 metals such as Cu, Zn and Pb, which are able to fix nitrogen to form complexes (Wuana
382 et al., 2010). Percentages of C and H were similar in each biomass section and soil.

383 The ICP-OES analysis showed that plants mainly absorbed and accumulated Fe (Table
384 5) because this was the predominant element in soils, although they also absorbed to a
385 less extent Cr, Ni, Cu, Zn and Pb. The concentrations of these metals found can be
386 considered as promising, since they were quite high. The concentration of Fe in plants
387 was higher than the accumulation limit by *J. curcas* for most metallic elements (1000 mg
388 kg^{-1}) reported by other authors (Ahmadpour et al., 2014; Ghavri and Singh, 2010).

389 The concentrations of Cu and Zn after 120 days were in the same range than those found
390 in *J. curcas* established for 105 days on a mine residue amended or not amended with
391 biochar and inoculated or not inoculated with the mycorrhizal fungus *Acaulospora* sp
392 (González-Chávez et al., 2017). By contrast, these authors found much lower
393 concentrations of Pb (less than 25 mg kg^{-1}) in their trials. Higher Cu concentrations (665
394 $\pm 1 \text{ mg kg}^{-1}$), based on total plant dry biomass, were found in *J. curcas* planted for 5

395 months in soils spiked with 400 mg kg⁻¹ Cu (Ahmadpour et al., 2014). However, our study
396 deals with much more contaminated soils with numerous heavy metals at high
397 concentrations at the same time, and the metal concentrations depend on plant growth. In
398 spite of achieving higher Cu concentrations in plant tissue, the maximum total Cu removal
399 from soils these authors achieved was 1.2% (Ahmadpour et al., 2014), while we achieved
400 Cu removal from soils of up to 72% (Table 4). Furthermore, *J. curcas* sowed in soils
401 artificially contaminated up to 10 mg Hg kg⁻¹ soil (using mercury nitrate solution) was
402 able to solely absorb up to 7.3 mg Hg kg⁻¹ biomass after 4-month trial (Marrugo-Negrete
403 et al., 2015). The low initial concentrations of trace elements (Cd, Hg and Sn) found in
404 the different parts of the plants (roots, stems and leaves) did not allow determining with
405 great precision their concentrations at the end of the heavy metal absorption trials. Since
406 these elements were not found in soils, it could be assumed that most of them were totally
407 absorbed by plants. Taken into account the different parts of the plant, 800.5, 633.3 and
408 872.1 mg metals kg⁻¹ plant were found in roots, stems and leaves, respectively, of
409 NCS100 samples; 1262.4, 1192.9 and 607.6 mg metals kg⁻¹ plant were found in roots,
410 stems and leaves, respectively, of YCS20 samples; and 2132.5, 446.4 and 421.2 mg
411 metals kg⁻¹ plant were found in roots, stems and leaves, respectively, of YCS50 samples.
412 As it can be observed, plants sowed in the most initially contaminated soil (YCS50) were
413 the ones that more metals accumulated in roots, which agrees with other authors' findings
414 (Ahmadpour et al., 2014; Ghavri and Singh, 2010; González-Chávez et al., 2017;
415 Marrugo-Negrete et al., 2015; Yadav et al., 2009). The first authors (Ghavri and Singh,
416 2010) detected 49.3 – 64.9 mg Fe kg⁻¹ *J. curcas* roots grown in garden soil for 100 days
417 while the Fe concentration in *J. curcas* roots grown in iron rich wasteland soil for 100
418 days was 6 folds higher (301.24 – 319.53 mg kg⁻¹). In our case, *Jatropha curcas* L. roots
419 sowed in SCN100, YCS20 and YCS50 soils for 120 days absorbed 622.2, 1124.3 and

420 1929.1 mg kg⁻¹ Fe.

421 Regarding the translocation of these metals in the plants, the metals are seen to remain
422 mainly in leaves and stems in most cases (Fig. 7). All the metals increased their
423 translocation to aerial parts of the plant over time for NSC100 and YCS20, except Cr in
424 plants sowed in NSC100 and Fe in plants sowed in YCS20. The metals translocation
425 factors for YCS50 showed and uneven behaviour, being the global translocation factor
426 for plants sowed in this soil lower than those for NCS100 and YSC20. The global
427 translocation factors (considering all the analysed metals) for NCS100, YCS20 and
428 YCS50 were 0.81, 1.95 and 1.37 at day 60, and 1.88, 1.43 and 0.41 at day 120,
429 respectively. Most of individual TF were higher than those found for the same plant for
430 Hg in mining soils artificially contaminated after the same phytoremediation time
431 (Marrugo-Negrete et al., 2015), for Cu in soils spiked with Cu in amounts of 0, 50, 100,
432 200, 300, and 400 mg kg⁻¹ (Ahmadpour et al., 2014), and for Cu, Zn and Pb in mining
433 soils with biochar addition and under the effect of mycorrhizal inoculation (González-
434 Chávez et al., 2017). Accumulation and distribution of heavy metals in plant tissues are
435 of major importance in phytoremediation of contaminated soils. If the objective is to
436 stabilize metals in roots for them not to enter in stems and leaves and therefore to prevent
437 metals from entering the ecosystem, low TF are desirable. Therefore, the low global TF
438 (0.41) obtained for the most contaminated soil (YCS50) at day 120 is a promising result.
439 On the contrary, the high TF obtained for some metals such as Cr, Ni, Zn and Pb cannot
440 be regarded as good results if the purpose is the phytoremediation of soils contaminated
441 with these metals.

442 With regard to bioaccumulation factors, in spite of the great Fe concentration absorbed by
443 plants (Table 5), BAF of Fe was very low for the 3 soils in the 2 days of sampling because
444 of the huge initial concentration of Fe (between 32213 and 265357 mg kg⁻¹), which could

445 not be removed in 120 days, so a great amount of Fe remained in the soils at the end of
446 this period of time (Table 4). This also led to low global bioaccumulation factors. The
447 global BAF for NCS100, YCS20 and YCS50 were 0.142, 0.097 and 0.041 at day 60, and
448 0.117, 0.083 and 0.049 at day 120, respectively. As can be noted, BAF decreased over
449 time. This was due to the huge plant growth from day 60 to day 120 (Fig. 5). BAF (except
450 for Fe) were in the range of those found for Hg, Cu, Zn and Pb in mining soils with *J.*
451 *curcas* for a similar cultivation period (González-Chávez et al., 2017; Marrugo-Negrete
452 et al., 2015), these soils having initial metal concentrations much lower than those used
453 in this study, which highlights the good results achieved.

454

455 **3.4. Characterization of the catalytic carbons.**

456 Two main phases can be distinguished in the thermogravimetric curves obtained in the
457 pyrolysis of the contaminated root samples at different temperatures. Fig. 9 depicts the
458 weight losses obtained for the roots of plants sowed in YCS50 soil, which had the highest
459 concentration of heavy metals ($2132.5 \text{ mg kg}^{-1}$). The first, between room temperature and
460 $350 \text{ }^\circ\text{C}$, is the active zone and is related to the degradation of polymers of hemicellulose
461 and cellulose. The second phase, the passive zone, showed a decrease in the slope until
462 $600 \text{ }^\circ\text{C}$ as a result of the decomposition of lignin. Beyond this phase, the slope steepened
463 again due to the loss of mass caused by the total degradation of the biomass.

464 Fig. S3 shows the Raman spectra of the pyrolytic carbons for this sample obtained from
465 $300 \text{ }^\circ\text{C}$ to $650 \text{ }^\circ\text{C}$ and the spectrum of the standard graphite. For C-based materials
466 containing C- sp^2 sites, the most intense features can be observed at about 1582, 1350,
467 1620 and 2700 cm^{-1} , which are called G, D, D' and 2D (also G') (Reich and Thomsen,
468 2004; Tai et al., 2009; Veres et al., 2008; Viana and Marques, 2015). The G band appears
469 from a double degenerated phonon mode with E_{2g} symmetry, while the D and D' bands

470 emerge from the phonon modes with A_{1g} symmetry (Ferrari and Robertson, 2000;
471 Pimenta et al., 2007; Reich and Thomsen, 2004). The G band appears in all graphite
472 samples, while the D and D' bands only appear in the spectra of disordered samples, and
473 highly crystalline graphite does not show these bands. So, the D band is attributed to
474 disorders and defects in the graphite structure. Comparing the G-band ($\sim 1575 \text{ cm}^{-1}$) and
475 the D-band ($\sim 1355 \text{ cm}^{-1}$) obtained for pyrolytic carbons with that of commercial graphite
476 (Fig. S5), it can be observed that the sample pyrolysed at $550 \text{ }^\circ\text{C}$ is the one that presents
477 the intensity ratio of G and D bands, as well as their positions and widths, more similar
478 to those of graphite. Samples pyrolysed at temperature lower than $550 \text{ }^\circ\text{C}$ showed wider
479 bands that overlap each other while samples pyrolysed at temperatures higher than 550
480 $^\circ\text{C}$ showed lower intensity bands, leading to the formation of amorphous carbonaceous
481 materials.

482 **Conclusions**

483 The high percentage of germination obtained from the seeds of *Jatropha curcas* L. (85%)
484 and the rapid adaptation to the spring climate simulated in the greenhouse make this
485 species a plant with wide possibilities for phytoremediation of marginal soils.
486 Nevertheless, *J. curcas* L. did solely survive in soil mixtures containing up to 50% of the
487 highly contaminated mining soils assayed in this work.

488 With regard to metal removal from soils, metals with low initial concentrations ($<10 \text{ mg}$
489 kg^{-1}) such as Hg, Sn and Cd were completely removed, while the concentrations of metals
490 within the range $10 - 1000 \text{ mg kg}^{-1}$ (Cr, Ni, Cu, Zn and Pb) were reduced between 30 –
491 70%, except As. The concentration of Fe in soils was solely reduced 15% as consequence
492 of its high initial concentration ($> 30000 \text{ mg kg}^{-1}$). On the other hand, the translocation

493 factors of Cr, Ni, Zn and Pb were high, which can be a hindrance for the phytoremediation
494 of soils containing high concentrations of these metals.
495 Finally, the structural characterization by Raman spectroscopy of pyrolytic coal obtained
496 from the contaminated roots of the *J. curcas* L. showed that the most suitable pyrolysis
497 temperature to obtain a graphite structure was 550 °C.

498

499 **Acknowledgments**

500 Authors gratefully thank Camposur Investiga S.L. for its financial support to this research
501 work

502

503 **References**

- 504 Abhilash, P.C., Powell, J.R., Singh, H.B., Singh, B.K., 2012. Plant-microbe
505 interactions: Novel applications for exploitation in multipurpose remediation
506 technologies. Trends Biotechnol. <https://doi.org/10.1016/j.tibtech.2012.04.004>
- 507 Abhilash, P.C., Singh, B., Srivastava, P., Schaeffer, A., Singh, N., 2013. Remediation of
508 lindane by *Jatropha curcas* L: Utilization of multipurpose species for
509 rhizoremediation. Biomass and Bioenergy 51, 189–193.
510 <https://doi.org/10.1016/j.biombioe.2013.01.028>
- 511 Ahmadpour, P., Soleimani, M., Ahmadpour, F., Abdu, A., 2014. Evaluation of Copper
512 Bioaccumulation and Translocation in *Jatropha curcas* Grown in a Contaminated
513 Soil. Int. J. Phytoremediation 16, 454–468.
514 <https://doi.org/10.1080/15226514.2013.798614>
- 515 Ali, Q., Ahsan, M., Khaliq, I., Elahi, M., Ali, S., Ali, F., Naees, M., 2011. Role of
516 Rhizobacteria in phytoremediation of heavy metals: An overview. Int. Res. J. Plant
517 Sci. 2, 220–232.

518 APHA, AWWA, WEF, 2005. Standard methods for the examination of water and
519 wastewater. Am. Public Heal. Assoc. Washington, DC, USA 1–2671.

520 Bernabé-Antonio, A., Álvarez, L., Buendía-González, L., Maldonado-Magaña, A.,
521 Cruz-Sosa, F., 2015. Accumulation and tolerance of Cr and Pb using a cell
522 suspension culture system of *Jatropha curcas*. *Plant Cell. Tissue Organ Cult.* 120,
523 221–228. <https://doi.org/10.1007/s11240-014-0597-y>

524 Chang, F.-C., Ko, C.-H., Tsai, M.-J., Wang, Y.-N., Chung, C.-Y., 2014.
525 Phytoremediation of heavy metal contaminated soil by *Jatropha curcas*.
526 *Ecotoxicology* 23, 1969–1978. <https://doi.org/10.1007/s10646-014-1343-2>

527 Chavan, S.B., Kumbhar, R.R., Madhu, D., Singh, B., Sharma, Y.C., 2015. Synthesis of
528 biodiesel from *Jatropha curcas* oil using waste eggshell and study of its fuel
529 properties. *RSC Adv.* 5, 63596–63604. <https://doi.org/10.1039/C5RA06937H>

530 Cobbett, C., 2003. Heavy metals and plants - Model systems and hyperaccumulators.
531 *New Phytol.* <https://doi.org/10.1046/j.1469-8137.2003.00832.x>

532 Delwiche, C.C., Bryan, B.A., 1976. Denitrification. *Annu. Rev. Microbiol.* 30, 241–
533 262.

534 Einsle, O., Kroneck, P.M.H., 2004. Structural basis of denitrification. *Biol. Chem.* 385,
535 875–883. <https://doi.org/10.1515/BC.2004.115>

536 Ferrari, A., Robertson, J., 2000. Interpretation of Raman spectra of disordered and
537 amorphous carbon. *Phys. Rev. B - Condens. Matter Mater. Phys.* 61, 14095–
538 14107. <https://doi.org/10.1103/PhysRevB.61.14095>

539 Ghavri, S.V., Singh, R.P., 2010. Phytotranslocation of Fe by biodiesel plant *Jatropha*
540 *curcas* L. grown on iron rich wasteland soil. *Brazilian J. Plant Physiol.* 22, 235–
541 243. <https://doi.org/10.1590/S1677-04202010000400003>

542 González-Chávez, M. del C.A., Carrillo-González, R., 2013. Tolerance of

543 Chrysanthemum maximum to heavy metals: The potential for its use in the
544 revegetation of tailings heaps. *J. Environ. Sci. (China)* 25, 367–375.
545 [https://doi.org/10.1016/S1001-0742\(12\)60060-6](https://doi.org/10.1016/S1001-0742(12)60060-6)

546 González-Chávez, M. del C.A., Carrillo-González, R., Hernández Godínez, M.I.,
547 Evangelista Lozano, S., 2017. *Jatropha curcas* and assisted phytoremediation of a
548 mine tailing with biochar and a mycorrhizal fungus. *Int. J. Phytoremediation* 19,
549 174–182. <https://doi.org/10.1080/15226514.2016.1207602>

550 Jackson, M.L., 1958. *Soil chemical analysis*. New York Prentice Hall 498.

551 Jamil, S., Abhilash, P.C., Singh, N., Sharma, P.N., 2009. *Jatropha curcas*: A potential
552 crop for phytoremediation of coal fly ash. *J. Hazard. Mater.* 172, 269–275.
553 <https://doi.org/10.1016/j.jhazmat.2009.07.004>

554 Järup, L., 2003. Hazards of heavy metal contamination. *Br. Med. Bull.* 68, 167–182.
555 <https://doi.org/10.1093/bmb/ldg032>

556 Jiménez-Moraza, C., Iglesias, N., Palencia, I., 2006. Application of sugar foam to a
557 pyrite-contaminated soil. *Miner. Eng.* 19, 399–406.
558 <https://doi.org/10.1016/j.mineng.2005.10.011>

559 LeDuc, D.L., Terry, N., 2005. Phytoremediation of toxic trace elements in soil and
560 water, in: *Journal of Industrial Microbiology and Biotechnology*. pp. 514–520.
561 <https://doi.org/10.1007/s10295-005-0227-0>

562 Marrugo-Negrete, J., Durango-Hernández, J., Pinedo-Hernández, J., Olivero-Verbel, J.,
563 Díez, S., 2015. Phytoremediation of mercury-contaminated soils by *Jatropha*
564 *curcas*. *Chemosphere* 127, 58–63.
565 <https://doi.org/10.1016/j.chemosphere.2014.12.073>

566 Mukhopadhyay, S., Maiti, S.K., 2010. Phytoremediation of metal mine waste. *Appl.*
567 *Ecol. Environ. Res.* 8, 207–222.

568 Pandey, V.C., Singh, K., Singh, J.S., Kumar, A., Singh, B., Singh, R.P., 2012. *Jatropha*
569 *curcas*: A potential biofuel plant for sustainable environmental development.
570 *Renew. Sustain. Energy Rev.* <https://doi.org/10.1016/j.rser.2012.02.004>

571 Pimenta, M.A., Dresselhaus, G., Dresselhaus, M.S., Cañado, L.G., Jorio, A., Saito, R.,
572 2007. Studying disorder in graphite-based systems by Raman spectroscopy. *Phys.*
573 *Chem. Chem. Phys.* 9, 1276–1290. <https://doi.org/10.1039/B613962K>

574 Reich, S., Thomsen, C., 2004. Raman spectroscopy of graphite. *Philos. Trans. R. Soc. A*
575 *Math. Phys. Eng. Sci.* 362, 2271–2288. <https://doi.org/10.1098/rsta.2004.1454>

576 Sánchez-Chardi, A., Ribeiro, C.A.O., Nadal, J., 2009. Metals in liver and kidneys and
577 the effects of chronic exposure to pyrite mine pollution in the shrew *Crocidura*
578 *russula* inhabiting the protected wetland of Doñana. *Chemosphere* 76, 387–394.
579 <https://doi.org/10.1016/j.chemosphere.2009.03.036>

580 Simón, M., Ortiz, I., García, I., Fernández, E., Fernández, J., Dorronsoro, C., Aguilar, J.,
581 1999. Pollution of soils by the toxic spill of a pyrite mine (Aznalcollar, Spain). *Sci.*
582 *Total Environ.* 242, 105–115. [https://doi.org/10.1016/S0048-9697\(99\)00378-2](https://doi.org/10.1016/S0048-9697(99)00378-2)

583 Singh, R., Gautam, N., Mishra, A., Gupta, R., 2011. Heavy metals and living systems:
584 An overview. *Indian J. Pharmacol.* 43, 246. [https://doi.org/10.4103/0253-](https://doi.org/10.4103/0253-7613.81505)
585 [7613.81505](https://doi.org/10.4103/0253-7613.81505)

586 Singh, O. V., Labana, S., Pandey, G., Budhiraja, R., Jain, R.K., 2003.
587 *Phytoremediation: an overview of metallic ion decontamination from soil.* *Appl.*
588 *Microbiol. Biotechnol.* 61, 405–412. <https://doi.org/10.1007/s00253-003-1244-4>

589 Suresh, B., Ravishankar, G.A., 2004. *Phytoremediation—A Novel and Promising*
590 *Approach for Environmental Clean-up.* *Crit. Rev. Biotechnol.* 24, 97–124.
591 <https://doi.org/10.1080/07388550490493627>

592 Tai, F.C., Lee, S.C., Chen, J., Wei, C., Chang, S.H., 2009. *Multipeak fitting analysis of*

593 Raman spectra on DLCH film. *J. Raman Spectrosc.* 40, 1055–1059.
594 <https://doi.org/10.1002/jrs.2234>

595 Teo, S.H., Rashid, U., Taufiq-Yap, Y.H., 2014. Heterogeneous catalysis of
596 transesterification of jatropha curcas oil over calcium–cerium bimetallic oxide
597 catalyst. *RSC Adv.* 4, 48836–48847. <https://doi.org/10.1039/C4RA08471C>

598 Teo, S.H., Taufiq-Yap, Y.H., Rashid, U., Islam, A., 2015. Hydrothermal effect on
599 synthesis, characterization and catalytic properties of calcium methoxide for
600 biodiesel production from crude *Jatropha curcas*. *RSC Adv.* 5, 4266–4276.
601 <https://doi.org/10.1039/C4RA11936C>

602 Tripathi, R.D., Srivastava, S., Mishra, S., Singh, N., Tuli, R., Gupta, D.K., Maathuis,
603 F.J.M., 2007. Arsenic hazards: strategies for tolerance and remediation by plants.
604 *Trends Biotechnol.* <https://doi.org/10.1016/j.tibtech.2007.02.003>

605 Veres, M., Tóth, S., Koós, M., 2008. New aspects of Raman scattering in carbon-based
606 amorphous materials. *Diam. Relat. Mater.* 17, 1692–1696.
607 <https://doi.org/10.1016/j.diamond.2008.01.110>

608 Viana, G.A., Marques, F.C., 2015. Raman and thermal desorption spectroscopy
609 analyses of amorphous graphite-like carbon films with incorporated xenon.
610 *Vacuum* 112, 17–24. <https://doi.org/10.1016/j.vacuum.2014.10.019>

611 Wuana, R.A., Okieimen, F.E., Imborvungu, J.A., 2010. Removal of heavy metals from
612 a contaminated soil using organic chelating acids. *Int. J. Environ. Sci. Technol.* 7,
613 485–496. <https://doi.org/10.1007/BF03326158>

614 Yadav, S.K., Juwarkar, A.A., Kumar, G.P., Thawale, P.R., Singh, S.K., Chakrabarti, T.,
615 2009. Bioaccumulation and phyto-translocation of arsenic, chromium and zinc by
616 *Jatropha curcas* L.: Impact of dairy sludge and biofertilizer. *Bioresour. Technol.*
617 100, 4616–4622. <https://doi.org/10.1016/j.biortech.2009.04.062>

618 Yee, K.F., Wu, J.C.S., Lee, K.T., 2011. A green catalyst for biodiesel production from

619 jatropha oil: Optimization study. *Biomass and Bioenergy* 35, 1739–1746.

620 <https://doi.org/10.1016/j.biombioe.2011.01.017>

621

Table 1. Percentages of non-contaminated soil from Cobre las Cruces mine (NCS) and grey (GCS) and yellow (YCS) contaminated soils from Aznalcóllar mine and pH of the resulting soil mixtures used to assess adaptation of *Jathopa curcas* L. to these soils.

Sample	NCS	GCS	YCS	pH
	(%)	(%)	(%)	
V100	0	0	0	7.00 ± 0.10 ^a
NCS100	100	0	0	7.47 ± 0.08 ^b
GCS20	80	0	20	4.54 ± 0.08 ^c
GCS50	50	0	50	3.50 ± 0.05 ^d
GCS80	20	0	80	1.56 ± 0.03 ^e
YCS20	80	20	0	4.60 ± 0.07 ^c
YCS50	50	50	0	2.58 ± 0.03 ^f
YCS80	20	80	0	2.14 ± 0.05 ^g
GYCS25	50	25	25	2.76 ± 0.02 ^h

Different lowercase letters in the pH column indicate significant differences according to ANOVA ($p \leq 0.05$).

Table 2. Concentration of trace elements in Cobre las Cruces and Aznalcóllar mine soils and maximum values proposed for a soil to be declared contaminated in Andalusia (Simón et al., 1999).

Metal (mg kg ⁻¹)	Andalusia soils		Cobre las Cruces mine	Aznalcóllar mine	
	pH < 7	pH > 7	NCS	GCS	YCS
Cd	< 2	< 3	6 ± 1 ^a	27 ± 3 ^b	13 ± 2 ^c
Cr	< 100		59 ± 3 ^a	8 ± 1 ^b	11 ± 1 ^c
Cu	< 40	< 100	40 ± 2 ^a	270 ± 15 ^b	585 ± 29 ^c
Ni	< 40	< 50	23 ± 1 ^a	12 ± 1 ^b	14 ± 1 ^c
Zn	< 200	< 500	102 ± 5 ^a	2608 ± 124 ^b	2485 ± 124 ^b
Pb	< 100	< 200	94 ± 5 ^a	48686 ± 2450 ^b	4557 ± 228 ^c
As	< 20		18 ± 1 ^a	2366 ± 112 ^b	1121 ± 56 ^c
Hg	< 1		0 ± 0 ^a	58 ± 2 ^b	19 ± 1 ^c
Sn	<20		0 ± 0 ^a	14 ± 2 ^b	5 ± 1 ^c

Averages with different lowercase letters in the same row are significantly different ($p \leq 0.05$).

Table 3. Content in carbonates (CaCO_3), phosphates (PO_4^{3-} or HPO_4^{2-}), nitrates (NO_3^-) and organic matter of NCS, GCS and YCS samples.

Soil	Carbonates (%)	Phosphates (mg kg⁻¹)	Nitrates (mg kg⁻¹)	Organic matter (g kg⁻¹)
NCS	11.8 ± 0.1 ^a	16.8 ± 0.4 ^a	13.2 ± 0.4 ^a	12 ± 2 ^a
GCS	0 ± 0.0 ^b	0.12 ± 0.1 ^b	837 ± 9.0 ^b	72 ± 17 ^b
YCS	0 ± 0.0 ^b	9.1 ± 0.3 ^c	1093 ± 63.0 ^c	22 ± 1 ^c

Averages with different lowercase letters in the same column are significantly different ($p \leq 0.05$).

Table 4. Decrease in the concentration of heavy metals in NCS100, YCS20 and YCS50 soils after 120 days.

% Concentration decrease			
Metal	NCS100	YCS20	YCS50
Cr	28	29	27
Fe	39	23	15
Ni	32	52	67
Cu	72	39	23
Zn	54	45	37
Cd	-	100	100
Hg	-	100	100
Sn	-	100	100
Pb	69	58	51
As	9	5	5

Table 5. Concentration of main heavy metals in plants sowed in NCS100, YCS20 and YCS50 soils after 60 and 120 days.

	Cr (mg kg ⁻¹)	Fe (mg kg ⁻¹)	Ni (mg kg ⁻¹)	Cu (mg kg ⁻¹)	Zn (mg kg ⁻¹)	Pb (mg kg ⁻¹)	Total (mg kg ⁻¹)
60 days							
NCS100	104.0 ± 0.0 ^a	3308.1 ± 0.036 ^a	0.0 ± 0.0 ^a	97.9 ± 0.0 ^a	222.1 ± 0.0 ^a	12.0 ± 0.0 ^a	3744.2
YCS20	33.8 ± 0.0 ^b	3130.5 ± 0.050 ^b	35.8 ± 0.0 ^b	44.0 ± 0.1 ^b	160.8 ± 0.0 ^b	139.8 ± 0.0 ^b	3544.8
YCS50	74.5 ± 0.0 ^c	2114.4 ± 0.015 ^c	23.8 ± 0.0 ^c	54.4 ± 0.0 ^c	305.4 ± 0.0 ^c	31.4 ± 0.0 ^c	2603.9
120 days							
NCS100	166.4 ± 0.0 ^d	1653.1 ± 0.014 ^d	76.0 ± 0.0 ^d	41.1 ± 0.0 ^d	203.1 ± 0.0 ^d	166.1 ± 0.0 ^d	2305.9
YCS20	119.6 ± 0.0 ^e	2503.7 ± 0.041 ^e	74.8 ± 0.0 ^e	40.4 ± 0.0 ^e	226.7 ± 0.0 ^e	97.8 ± 0.0 ^e	3062.9
YCS50	49.76 ± 0.0 ^f	2598.2 ± 0.015 ^f	19.5 ± 0.0 ^f	44.5 ± 0.0 ^f	242.0 ± 0.0 ^f	46.3 ± 0.0 ^f	3000.2

Averages with different lowercase letters in the same column are significantly different ($p \leq 0.05$).

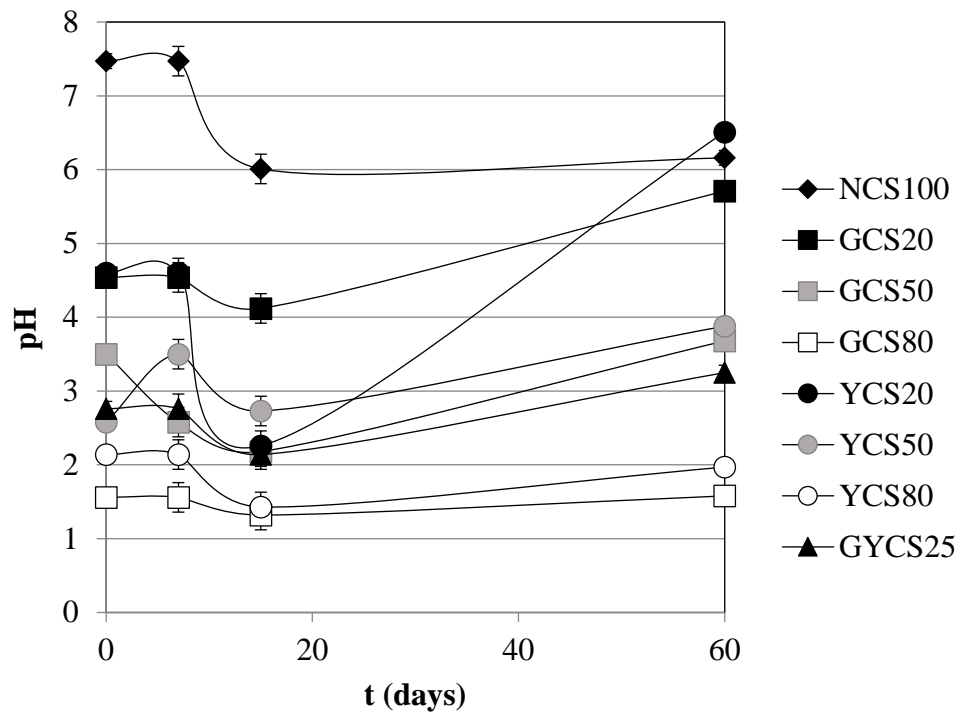


Figure 1: Evolution of pH over time for each soil sample assayed in the preliminary trials.

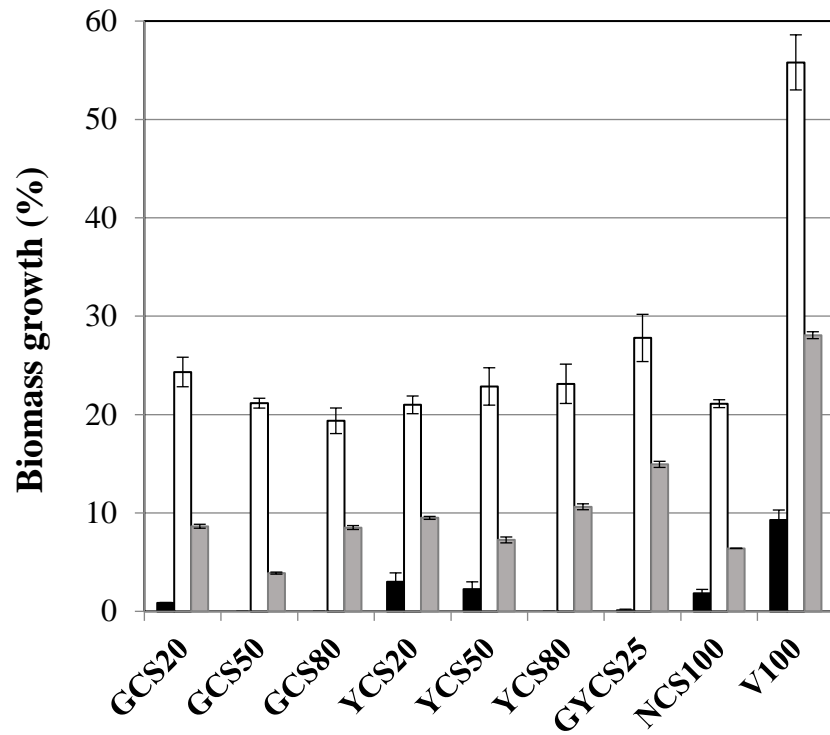


Figure 2. Percentage of growth of leaves (black bars), stems (open bars) and roots (grey bars) of *Jatropha curcas* L. in each soil at the end of the 60-day adaptation period.

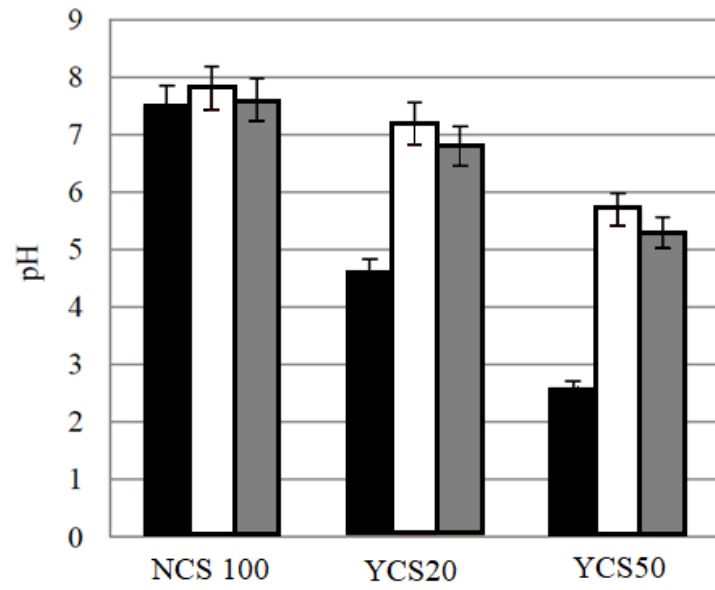


Figure 3: Changes in pH in soils at days 0 (black bars), 60 (open bars) and 120 (grey bars) during the heavy metal absorption trials.

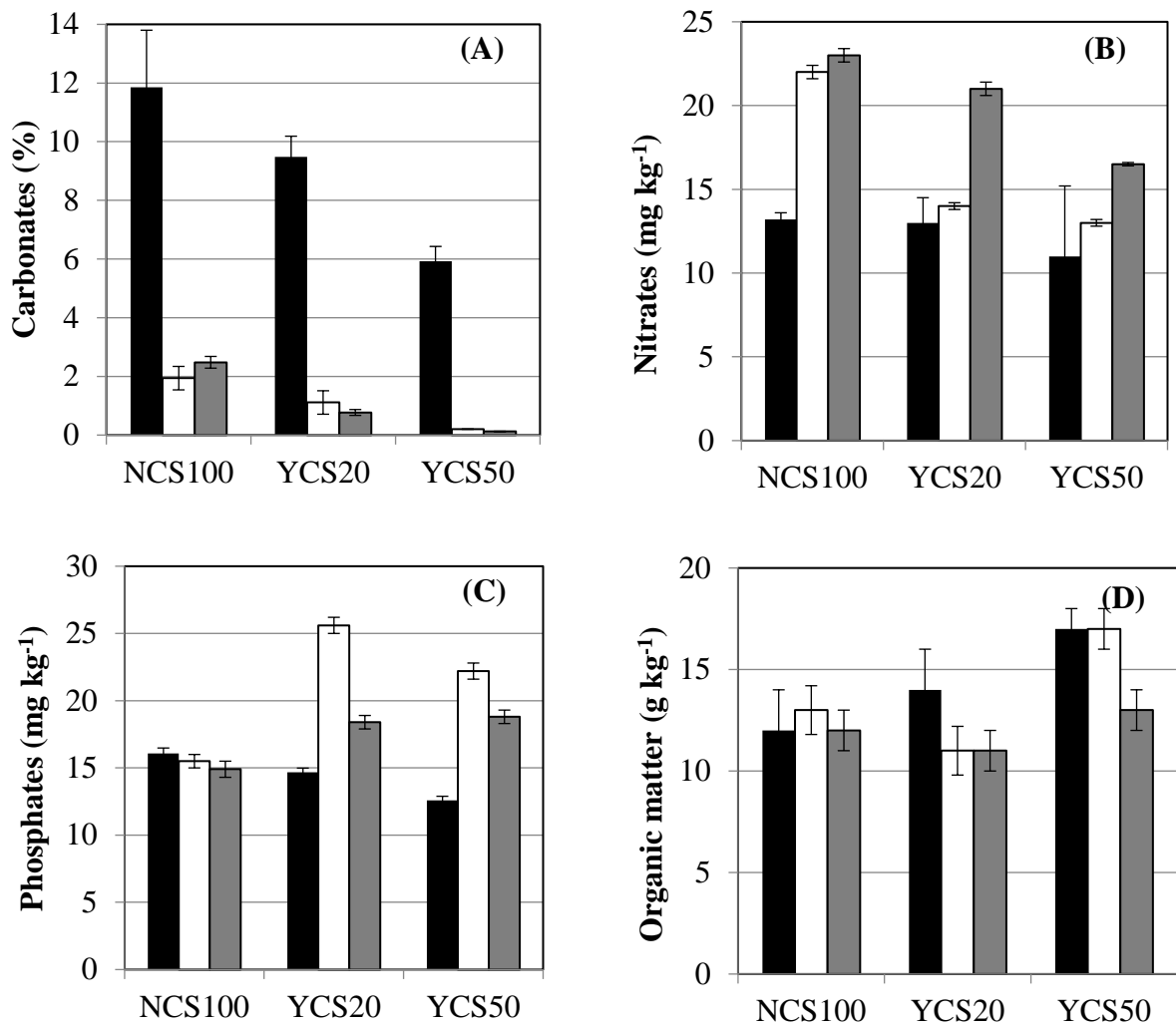


Figure 4: Evolution of the contents of (A) carbonates, (B) phosphates, (C) nitrates and (D) organic matter in NCS100, YCS20 and YCS50 soils at the beginning (black bars), after 60 days (open bars) and after 120 days (grey bars).

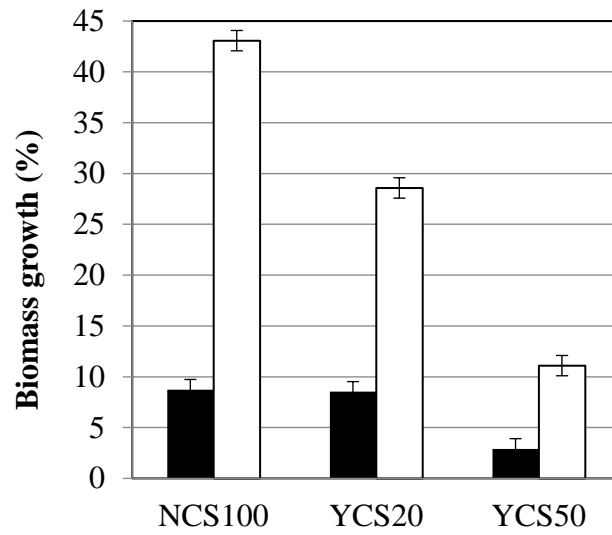


Figure 5: Percentage of biomass increased of plants sowed in NCS100, YCS20 and YCS50 soils after 60 (black bars) and 120 (open bars) days.

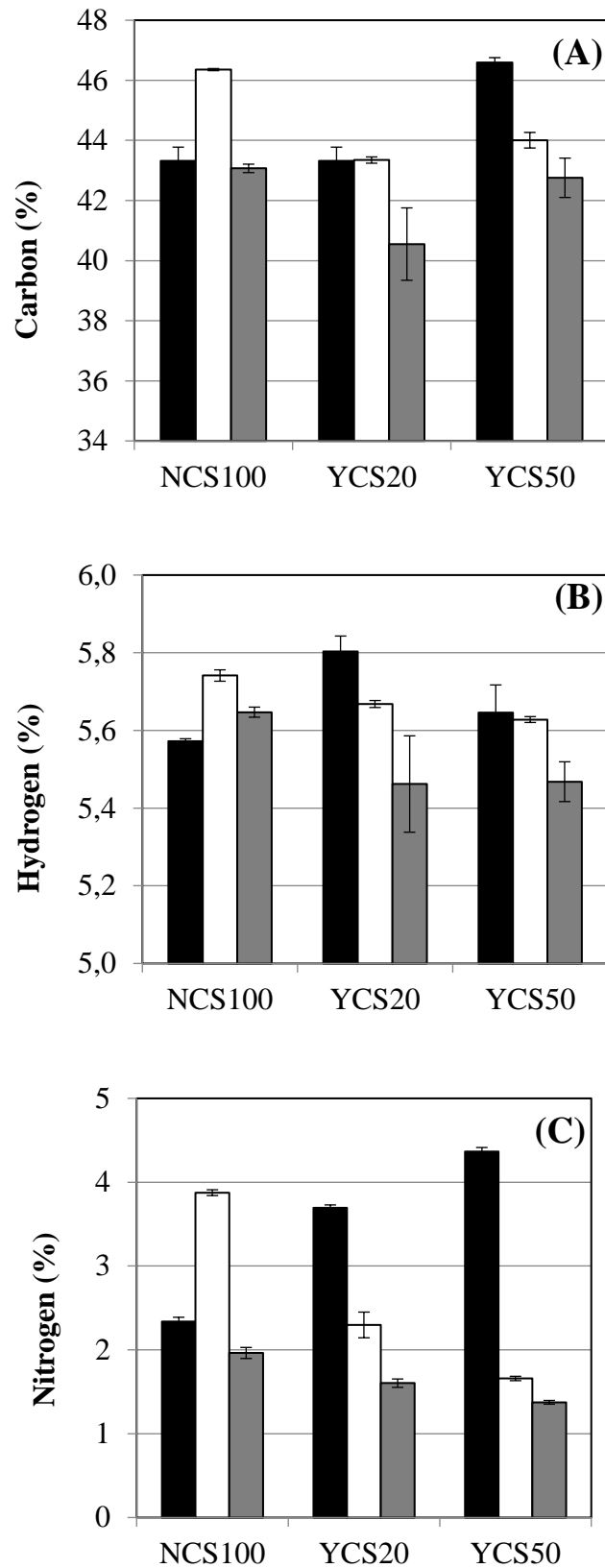


Figure 6. Elemental analysis of carbon (A), hydrogen (B) and nitrogen (C) in leaves (black bars), stems (open bars) and roots (grey bars) of plants sowed for 120 days in

NCS100, YCS20 and YCS50 soils.

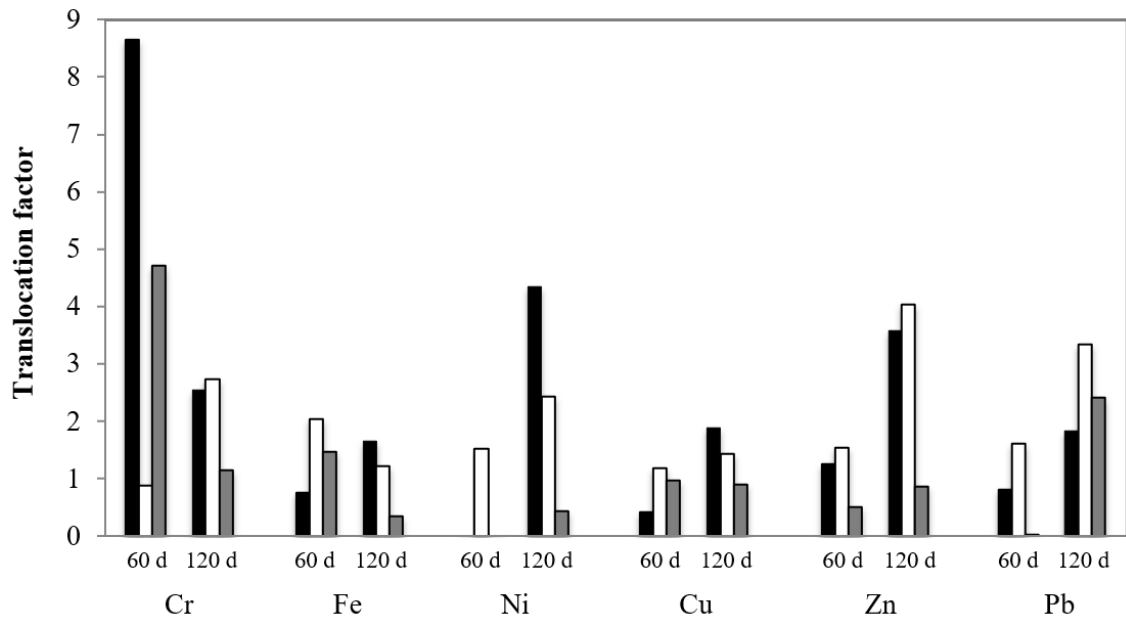


Fig. 7: Translocation factors of Cr, Fe, Ni, Cu, Zn and Pb of *Jatropha curcas* L. plants sowed in NCS100 (black bars), YSC20 (open bars) and YCS50 (grey bars) soils after 60 and 120 days.

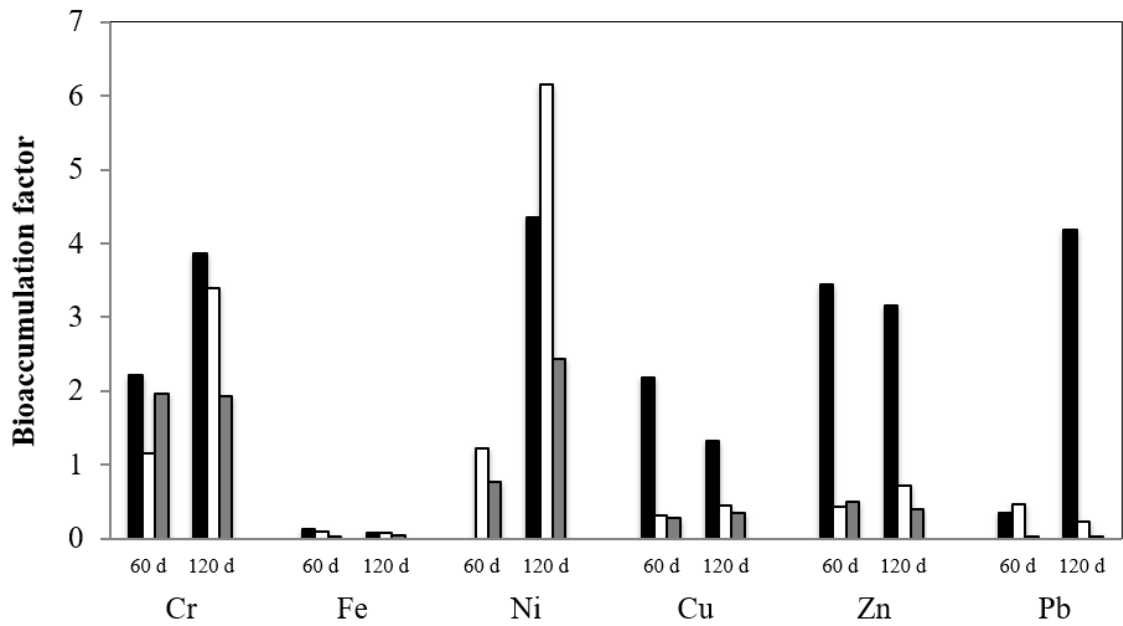


Fig. 8: Bioaccumulation factors of Cr, Fe, Ni, Cu, Zn and Pb of *Jatropha curcas* L. plants sowed in NCS100 (black bars), YSC20 (open bars) and YCS50 (grey bars) soils after 60 and 120 days.

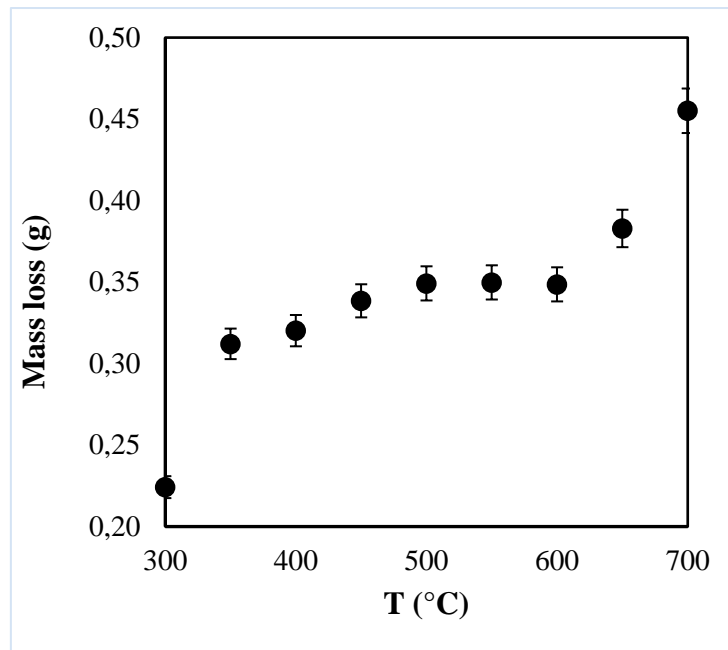


Figure 9. Thermogravimetric curve obtained in the pyrolysis of the roots of *Jatropha curcas* L. planted in the YCS50 soil.